Crystallographic Analysis of a Hydroxylated Polychlorinated Biphenyl (OH-PCB) Bound to the Catalytic Estrogen Binding Site of Human Estrogen Sulfotransferase

Sergei Shevtsov,[1] Evgeniy V. Petrotchenko,[1] Lars C. Pedersen,[1,2] and Masahiko Negishi[1]

[1]Pharmacogenetic Section, Laboratory of Reproductive and Developmental Toxicology, and [2]Laboratory of Structural Biology, National Institute of Environmental Health Sciences, Research Triangle Park, North Carolina, USA

Certain hydroxylated polychlorinated biphenyls (OH-PCBs) inhibit the human estrogen sulfotransferase (hEST) at subnanomolar concentrations, suggesting a possible pathway for PCB toxicity due to environmental exposure in humans. To address the structural basis of the inhibition, we have determined the crystal structure of hEST in the presence of the sulfuryl donor product 3′-phosphoadenosine 5′-phosphate and the OH-PCB 4,4′-OH 3,5,3′,5′-tetraCB. The OH-PCB binds in the estrogen binding site with the position of the first phenolic ring in an orientation similar to the phenolic ring of 17β-estradiol. Interestingly, the OH-PCB does not bind in a planar conformation, but rather with a 30-degree twist between the phenyl rings. The crystal structure of hEST with the OH-PCB bound gives physical evidence that certain OH-PCBs can mimic binding of estrogenic compounds in biological systems. *Key words:* crystal structure, estrogen, PCB, polychlorinated biphenyl, sulfotransferase. *Environ Health Perspect* 111:884–888 (2003). doi:10.1289/ehp.6056 available via *http://dx.doi.org/* [Online 12 February 2003]

Estrogen sulfotransferase (EST) is a cytosolic sulfotransferase that transfers a sulfuryl group from the ubiquitous sulfate donor 3′-phospho-adenosine 5′-phosphosulfate (PAPS) to the 3-hydroxyl on 17β-estradiol (E2). The sulfonation of E2 makes the compound more soluble for renal excretion as well as for the creation of inactive stores of sulfated E2 that can be desulfated by steroid sulfatases (Coughtrie et al. 1998). Both the estrogen receptor (ER) and EST have affinities for E2 in the nanomolar range, thus suggesting that EST may play an important role in the regulation of estrogenic effects by controlling the levels of E2 (Adams 1991; Falany and Falany 1996). The ability of EST to mediate local estrogen concentration has been demonstrated in mice by gene disruption studies (Qian et al. 2001; Tong and Song 2002).

Recently, it has been shown that some hydroxylated polychlorinated biphenyls (OH-PCBs) can inhibit human EST (hEST) (Kester et al. 2000). PCBs are persistent man-made environmental pollutants found in terrestrial and aquatic systems. These compounds and their metabolites accumulate in mammals and have been suggested to be endocrine disruptors based on links with disturbance of sexual development and reproductive function (Brouwer et al. 1999; Cheek et al. 1998). The pathway by which these compounds exert their toxic effect is not well understood. However, the OH-PCBs (4-OH-PCBs especially) share structural similarities, such as a phenolic ring, with E2 and may exert their endocrine effects by mimicking E2 binding to various proteins. Many endocrine disruptors exert their toxic effects through interactions with the ER. It has previously been demon-strated that PCB metabolites can bind the ER (Connor et al. 1997; Korach et al. 1988). Some PCB metabolites such as OH-PCBs and PCB-catechols are capable of stimulating *in vitro* translocation of ER into the nucleus and binding to the ER response elements (Connor et al. 1997; Garner et al. 1999; Korach et al. 1997). However, the concentrations required to elicit this response is two to three orders of magnitude greater than E2, thus questioning the significance of this pathway for endocrine disruption in the presence of physiologically relevant amounts of PCBs accumulated from environmental exposure.

Interestingly, PCBs inhibit hEST with IC_{50} (concentration that inhibits 50%) values as low as 0.1 nM (Kester et al. 2000). This level is roughly 40-fold lower than the K_m for the substrate E2. Thus, the study by Kester et al. suggests that a possible mechanism for endocrine disruption by PCBs and their hydroxylated metabolites may be an indirect effect whereby inhibition of hEST by OH-PCBs enhances estrogenic activity by increasing the levels of E2 in target tissues.

Based on Lineweaver-Burk plots, Kester et al. (2000) suggest that the inhibition by OH-PCBs appears to be noncompetitive. Based on kinetic data, it has previously been reported that hEST may contain an allosteric site (Zhang et al. 1998). Therefore, Kester et al. proposed that the mode of inhibition may be due to OH-PCB binding to this allosteric site (Kester et al. 2000).

To address the question of how OH-PCBs interact with hEST, we have determined the crystal structure of hEST in complex with the sulfuryl donor product PAP and with the most effective inhibitor reported by Kester et al., 4,4′-OH-3,5,3′,5′-tetraCB (Kester et al. 2000). Previously we determined the crystal structures of hEST in the presence of the sulfuryl donor PAPS and in complex with PAP (donor product) and E2 (Pedersen et al. 2002). In the E2 complex structure, the E2 molecule is bound in a hydrophobic pocket with the acceptor 3-hydroxyl within hydrogen bonding distance to histidine 107, the proposed catalytic base (Kakuta et al. 1997; Pedersen et al. 2002). This positions the 3-hydroxyl for an in-line nucleophilic attack on the sulfur atom of PAPS to form the sulfated product. In this study we found 4,4′-OH-3,5,3′,5′-tetraCB in the active site binding in the same position as the E2 substrate. Such binding suggests competitive inhibition. Although we do not attempt to validate the role or mode of endocrine disruption by PCBs and their metabolites, this study clearly shows that certain OH-PCBs are capable of mimicking E2 binding to hEST.

Materials and Methods

Protein for the wild-type hEST was expressed and purified as previously described for the V269E mutant (Pedersen et al. 2002). We obtained crystals of hEST using the sitting drop vapor diffusion technique. Protein concentrated at 15 mg/mL in 0.5 mM monosodium phosphate, 100 mM sodium chloride, and 4 mM PAP at pH 7.5 was mixed in equal volume with 0.1 M 2-[*N*-morpholino]ethane sulfonic acid, pH 6.0, and 18% polyethylene glycol 8000, then placed at 20°C. Typical crystals appeared after 10 days and grew to 0.5 mm × 0.5 mm × 0.02 mm after 1 month. For data collection, crystals were transferred to 0.1 M 2-[*N*-morpholino]ethane sulfonic acid, pH 6.0, 22% polyethylene glycol 8000, and 4 mM PAP, followed by an overnight soak in either saturated 1,3,5 (10)-estratrien-2,4-dibromo-3,17β-diol (E2Br$_2$) or 4,4′-OH-3,5,3′,5′-tetraCB. Crystals were then transferred in four steps of increasing ethylene

glycol concentration until a final concentration of 15% ethylene glycol in the soaking solution was obtained. The crystals were flash-frozen in a nitrogen stream at –180°C. Data were collected on a RaxisIV image plate detector with a RU3H rotating anode generator (Rigaku/MSC Inc., Woodlands, TX) (Table 1). All data were processed using Denzo and Scalepack programs (Otwinowski and Minor 1997). Coordinates with Protein Data Bank (PDB) identification code of 1HY3 of the V269E mutant of hEST were used as the starting coordinates for refinement. The program "O" was used for model building (Jones et al. 1991) and CNS for refinement (Brünger et al. 1998). We checked the quality of the models using PROCHECK (Table 1) (Bailey 1994). Coordinates for E2Br$_2$ and PCB were obtained from the Cambridge Structural Data Base (Cody et al. 1971; McKinney and Singh 1988). The coordinates have been submitted to the PDB and given the PDB identification code 1G3M.

Results

In the crystal structure of hEST in the presence of PAP and E2, the E2 molecule is located in a hydrophobic substrate binding pocket (Pedersen et al. 2002). The acceptor 3-hydroxyl group is located 2.6 Å from NZ of K105 and 2.8 Å from NE2 of H107 [single letter abbreviation code used for amino acid residues (i.e., histidine 107 = H107;); atom names used are based on PDB format]. Residues lining the substrate binding pocket near the active site include H107, K105, Y168, Y239, F141, F23, M247, Y81, V145, and C83. In this study, 4,4′-OH-3,5,3′,5′-tetraCB binds in the active site of hEST in a position similar to that of the E2 molecule (Figure 1). Like the E2 molecule, binding of 4,4′-OH-3,5,3′,5′-tetraCB appears to induce no obvious conformational change in residues lining the substrate binding pocket. Superposition of the protein molecules from the hEST + PAP + 4,4′-OH-3,5,3′,5′-tetraCB to that of hEST + PAP + E2 places the 4-hydroxyl group of the OH-PCB in a location similar to the 3-hydroxyl of E2, but offset approximately 1 Å from its position (Figure 2). The 4-hydroxyl group is 3.1 Å from NZ of K105 and 2.8 Å from NE2 of H107 (Figures 1A, 3B). Thus the 4-hydroxyl of the inhibitor is able to form the same interactions with these residues as the 3-hydroxyl of the acceptor substrate E2 (Figures 3B, 3C) (Pedersen et al. 2002). The phenol ring containing the 4-hydroxyl is also shifted 1 Å with respect to the A ring of the E2, and the plane of the ring is raised out of the plane of the A ring of E2 by about 12° (Figure 2A). The remaining phenol ring of 4,4′-OH-3,5,3′,5′-tetraCB is rotated ~30° out of the plane of the first ring (Figure 2C). The 4′-hydroxyl is located 3.1 Å from A146 and

2.9 Å from a water molecule that is also 2.8 Å from OD2 of D22 (Figures 1B, 3A). These interactions with the 4′-hydroxyl might help to increase the binding affinity to hEST for this particular OH-PCB.

The torsion angle of 30° differs from that of the solid-state crystal structure, which is a coplanar structure (torsion angle 0°) (McKinney and Singh 1988). Interestingly, energy calculations for the possible torsion

Table 1. Crystallographic data statistics.

Data set	PAP + 4,4′-OH-3,5,3′,5′-tetraCB	PAP + E2Br$_2$
Unit cell dimensions	a = 62.69, b = 96.89, c = 61.72	a = 61.16, b = 96.97, c = 62.52
	α = 90°, β = 92.58°, δ = 90°	α = 90°, β = 92.70°, δ = 90°
Space group	P2$_1$	P2$_1$
No. of observations	151,066	139,656
Unique reflections	75,359	60,218
R$_{sym}$ (%) (last shell)[a]	5.8 (26.2)	5.2 (31.2)
$I/\sigma I$ (last shell)	8.4 (1.9)	9.7 (1.7)
Mosaicity	0.57	0.61
Completeness (%) (last shell)	92.6 (82.9)	88.8 (73.9)
Refinement statistics		
Resolution (Å)	50–1.7	50–1.8
R$_{cryst}$ (%)[b]	19.3	19.0
R$_{free}$[c]	21.9	22.0
No. of waters	603	469
RMSD from ideal values		
Bond length (Å)	0.006	0.006
Bond angle (°)	1.2	1.2
Dihedral angle (°)	21.1	21.0
Improper angle (°)	0.76	0.77
Mean B value (Å^2)	21.4	27.2
Ramachandran statistics		
Residues in		
Most-favored regions (%)	93.0	91.5
Additionally allowed regions	6.8	8.3
Generously allowed regions	0.0	0.0
Disallowed regions	0.2	0.2

Abbreviations: cryst, crystal; RMSD, root–mean–square deviation; sym, symmetry.
[a]R$_{sym}$ = Σ (| I_i – <I>|)/ Σ(I_i), where I_i is the intensity of the ith observation and <I> is the mean intensity of the reflection.
[b]R$_{cryst}$ = Σ|| Fo| – | Fc ||/ Σ| Fo| calculated from working data set. [c]R$_{free}$ is calculated from 5% of data randomly chosen not to be included in refinement.
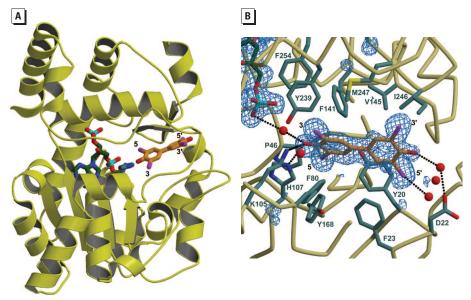

Figure 1. (*A*) Cartoon diagram of the crystal structure of human EST (yellow) in the presence of donor product PAP (green) and the PCB inhibitor 4,4′-OH-3,5,3′,5′-tetraCB (orange). The chlorides have been labeled 3, 3′, 5, and 5′. Also pictured is the proposed catalytic base H107 (blue). (*B*) Active site of hEST with 4,4′-OH-3,5,3′,5′-tetraCB bound. Side chains within 4.4 Å are displayed. The OH-PCB molecule is shown in orange, the PAP molecule in green, backbone trace in khaki, side chain atoms in blue, and water molecules as red spheres. The fo-fc annealed omit map for PAP and 4,4′-OH-3,5,3′,5′-tetraCB is shown contoured at 3σ (blue). Possible hydrogen bonds are represented with black dashed lines, and chlorides have been labeled as 3,3′5, and 5′. Figure 1 was created using MOLSCRIPT (Kraulis 1991) and RASTER3D (Merritt and Bacon 1997).

angles for the PCB 3,3′,4,4′,5,5′-hexaCB, similar to the one used in our study, suggest the energy minimum is at 42° with a maximum at 0° of 3.7 kcal/mol (McKinney et al. 1983). At 30°, the energy barrier is calculated to be around 0.4 kcal/mol, suggesting the torsion angle in the crystal structure for 4,4′-OH-3,5,3′,5′-tetraCB is in a lower energy orientation than in the solid-state crystal structure. The 30° torsion angle found in the protein crystal structure complex presented here is in good agreement with another energy calculation that predicts a minima in the torsion angle at 32° for an unsubstituted biphenyl (Almlöf 1974).

To examine what role the chlorines at positions 3 and 5 may have on the offset of the phenyl group nearest the active site, $E2Br_2$ was soaked into the crystal. $E2Br_2$ appears to bind in a location similar to that of E2, but is shifted in the direction of the 4,4′-OH-3,5,3′,5′-tetraCB, suggesting that the halides in the *ortho* position to the 4-hydroxyl may play a role in this shift (Figure 2). In addition, this result suggests that other halides such as Br can substitute for Cl at the positions adjacent to the hydroxyl on the phenol ring for binding to hEST.

Discussion

It has been suggested that 4,4′-OH-3,5,3′,5′-tetraCB is an extremely effective noncompetitive inhibitor to the hEST enzyme, with IC_{50} values in the low nanomolar range (Kester et al. 2000). Those studies indicate that the OH-PCBs may bind primarily to a proposed allosteric site. The current crystal structure, however, places the PCB molecule in the E2 position in the active site. Binding at this position implies competitive inhibition is to be expected. Although there has been no crystallographic evidence of an additional binding site in any EST structure, both the PAP + E2 and PAP + 4,4′-OH-3,5,3′,5′-tetraCB crystal structures were obtained by soaking the substrate or inhibitor into the preformed crystal. Therefore, if a major conformational change is

required for binding to the additional site, or if this site were positioned at a crystallographic interface, it is unlikely that we would observe binding. Consequently, the existence of this site cannot be ruled out. However, supporting the crystallographic data, previous inhibition studies of the sulfonation of 3,3′-diiodothyronine by cytosolic sulfotransferases using 4-OH-2′,3,3′,4′,5-pentaCB suggest the inhibition mechanism is competitive (Schuur et al. 1998).

In general, the position of the 4,4′-OH-3,5,3′,5′-tetraCB molecule in the hEST crystal structure is consistent with the IC_{50} results of the various PCB molecules tested by Kester et al. (2000). Using OH-PCBs with an identical 4-hydroxy-3,5-dichloro–substituted phenolic ring. Kester et al. noted that especially potent inhibition was observed for 3′,4′ substitution and 3′,5′ substitution with Cl atoms. The current orientation of 4,4′-OH-3,5,3′,5′-tetraCB bound to hEST could accommodate both of these types of substitution without major steric clashes. As shown by our crystal structure, substitutions at the 3-, 3′-, 5-, and 5′-positions are easily tolerated (Figures 2, 3A). Addition of chlorine atoms at the 3-, 3′-, 5-, and 5′-positions increases the surface area of the PCB molecule, which could allow for greater Van der Waal interactions between 4,4′-OH-3,5,3′,5′-tetraCB and hEST, thus increasing the binding affinity. In addition, positioning of a hydroxyl group at the 4-position would allow for strong hydrogen bonding interactions with the NZ atom of K105 and the NE2 atom of H107. The conformation and position of 4,4′-OH-3,5,3′,5′-tetraCB in the active site could allow for OH or Cl substitution at the 3,3′-, 4′-, 5-, 5′-, and possibly the 4-position. Chlorine atoms are capable of forming hydrogen bonds, but they are typically longer than N…H–O hydrogen bonds, suggesting a slight rearrangement in side chains 107 and 105, and possible slight positioning change of the molecule would be required for these compounds with chlorines in the 4-position to bind in the same orientation.

Other substitutions are also possible. Based on the current position, substitutions at the 2- or 2′-position can occur without large Van der Waal conflicts with the protein (Figure 3A). In addition, a slight change in the torsion angle to 45° from planar would lower the predicted rotational potential energy from 12 kcal/mol to 4 kcal/mol, which is the same rotational potential for the coplanar arrangement of an unsubstituted biphenyl (McKinney et al. 1983). However, substitution at the 6- or 6′-position would create large Van der Waal conflicts with Y20 (Figure 3A).

Based on the position of the 4,4′-OH-3,3′,3′,5′ tetraCB to hEST, models of six of the seven PCBs with the lowest IC_{50} values (IC_{50} < 1nM) can be easily accommodated. Molecules 4-OH-2,3,5,5′,3′,4′-pentaCB (IC_{50} 0.15–0.25nM), 4-OH-3,5′,3′,4′-tetraCB (IC_{50} 0.21–0.61nM), 4-OH-3,5,3′,5′-tetraCB (IC_{50} 0.47–1.0), 4-OH-3,5,2′,3′,4′-pentaCB (IC_{50} 0.28–0.30), and 4-OH-3,5,3′,4′,5′-pentaCB should all be able to fit into the active site with the same orientation as the 4,4′-OH-3,3′,3′,5′-tetraCB molecule used in this study. In addition, the seventh molecule 4-OH-2,3,5,2′,3′,4′-hexaCB (IC_{50} 0.27–0.75) might be able to bind without much change. A rotation of 180° of the second phenyl ring in Figure 3 would be required so the 2 and 2′ occupants would not create a bad steric contact. This conformation might cause a slight Van der Waal interaction between the 2′ Cl and Y20 that could possibly be alleviated by minor rearrangement of the molecule or side chains.

Using the same principles, all the remaining molecules with IC_{50} values < 50nM could also be accommodated, with one exception: molecule 4-OH-2,3,5,6,2′,4′,5′-heptaCB (IC_{50} 6.8–30). In general, the best inhibitors from the study of Kester et al. (2000) (IC_{50}s < 5nM) do not have substitution at the 2- and the 6-position. The 6-position Cl in the current orientation would have a major Van der Waal contact with Y20, and because there are
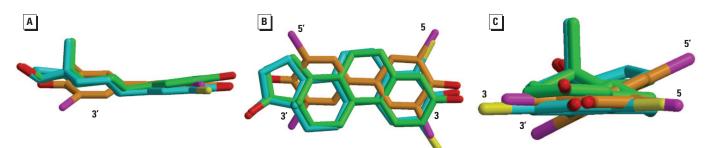

Figure 2. (*A*) Orientation of the ligands from the superposition of the complexes of hEST with 4,4′-OH-3,5,3′,5′-tetraCB (carbons orange, chlorides magenta), E2 (carbons green), $E2Br_2$ (carbons blue, bromines yellow) bound in the active site; this figure shows an approximate 12° shift of the PCB and $E2Br_2$ phenolic rings from that of the E2 substrate. (*B*) Rotation of (*A*) by approximately 90° along a horizontal axis; the phenolic ring of 4,4′-OH-3,5,3′,5′-tetraCB containing the 4 OH is slightly offset from the phenolic ring of the E2 substrate. (*C*) Rotation of (*A*) by 90° along a vertical axis; the 3 OH of E2 is located out of the plane of the page. (*C*) Clearly shows the approximate 30° twist in the second phenolic ring of 4,4′-OH-3,5,3′,5′-tetraCB from that of the first ring. The visible chlorides have been labeled in (*A*), (*B*), and (*C*). These figures were created using MOLSCRIPT (Kraulis 1991) and RASTER3D (Merritt and Bacon 1997).

three substitutions at the *ortho* positions (2,6,2′) on the phenyl rings, this molecule would most likely have to have a torsion angle near 90° between the two phenyl rings. Thus, the binding of this particular molecule cannot be explained by the current position of the PCB molecule.

In conclusion, these studies support the notion that certain OH-PCBs are capable of binding to hEST and inhibiting its function as shown by Kester et al. (2000). The OH-PCB molecule 4,4′-OH-3,5,3′,5′-tetraCB binds at the E2 binding position in the active site, suggesting competitive inhibition. Thus, for the

first time, the crystal structure of hEST in the presence of PAP and 4,4′-OH-3,5,3′,5′-tetraCB provides atomic detail of a hydroxylated PCB compound mimicking hormone binding to protein molecules.

Although it is not clear what effect environmental exposure to PCBs has on the proper function of hEST *in vivo*, the kinetic data by Kester et al. (2000), combined with the crystallography presented in this study, suggest that future studies are warranted.
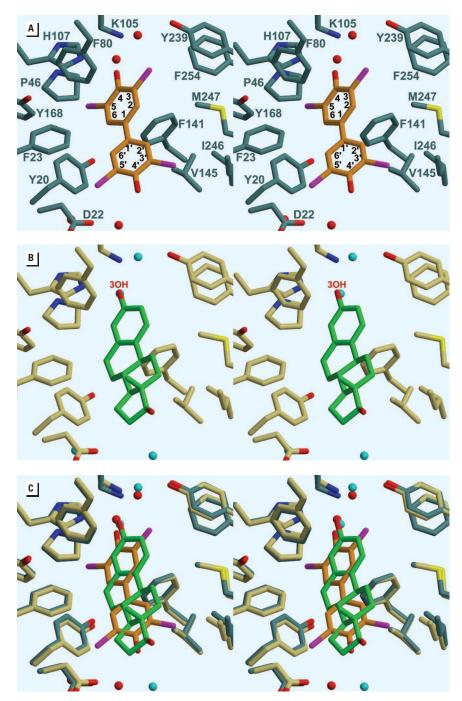

Figure 3. Stereo diagrams of the active sites of the crystal structures of hEST [figure created using MOLSCRIPT (Kraulis 1991) and RASTER3D (Merritt and Bacon 1997)]. (*A*) Active site of hEST with 4,4′-OH-3,5,3′,5′-tetraCB bound. Side chains, blue; 4,4′-OH-3,5,3′,5′-tetraCB, orange; chlorine atoms, magenta; water molecules, red. (*B*) Active site of hEST with E2 (green) bound to the active site. The acceptor hydroxyl of the E2 molecule has been labeled 3OH. Side chains for active site residues, khaki; water molecules, cyan. (*C*) Active sites of the crystal structures of hEST with 4,4′-OH-3,5,3′,5′-tetraCB and E2 bound. Side chains, blue in the structure with 4,4′-OH-3,5,3′,5′-tetraCB bound; water molecules, red, khaki, in the structure with E2 bound; water molecules, cyan.

REFERENCES

Adams JB. 1991. Enzymatic regulation of estradiol-17β concentrations in human breast cancer cells. Breast Cancer Res Treat 20:145–154.

Almlöf J. 1974. Ab initio calculations of the equilibrium geometry and rotation barriers in biphenyl. Chem Phys 6:135–139.

Bailey S. 1994. The CCP4 suite: programs for protein crystallography. Acta Crystallogr D 50:760–763.

Brouwer A, Longnecker MP, Birnbaum LS, Cogliano J, Kostyniak P, Moore J, et al. 1999. Characterization of potential endocrine-related health effects at low-dose levels of exposure to PCBs. Environ Health Perspect 107(suppl 4):639–649.

Brünger AT, Adams PD, Clore GM, DeLano WL, Gros P, Grosse-Kunstleve RW, et al. 1998. Crystallography & NMR system: a new software suite for macromolecular structure determination. Acta Crystallogr D 54:905–921.

Cheek AO, Vonier PM, Oberdorster E, Burow BC, McLachlan JA. 1998. Environmental signaling: a biological context for endocrine disruption. Environ Health Perspect 106(suppl 1):5–10.

Cody V, DeJarnette F, Duax W, Norton DA. 1971. Conformational change in two modifications of 2,4 dibromoestradiol. Acta Crystallogr Sect B 27:2458.

Connor K, Ramamoorthy K, Moore M, Mustain M, Chen I, Safe S, et al. 1997. Hydroxylated polychlorinated biphenyls (PCBs) as estrogens and antiestrogens: structure-activity relationships. Toxicol Appl Pharmacol 145:111–123.

Coughtrie MW, Sharp S, Maxwell K, Innes NP. 1998. Biology and function of the reversible sulfation pathway catalysed by human sulfotransferases and sulfatases. Chem Biol Interact 109:3–27.

Falany JL, Falany CN. 1996. Expression of cytosolic sulfotransferases in normal mammary epithelial cells and breast cancer cell lines. Cancer Res 56:1551–1555.

Garner CE, Jefferson WN, Burka LT, Matthews HB, Newbold RR. 1999. In vitro estrogenicity of the catechol metabolites of selected polychlorinated biphenyls. Toxicol Appl Pharmacol 154:188–197.

Jones TA, Zou JY, Cowan SW, Kjeldgaard M. 1991. Improved methods for building protein models in electron density maps and the location of errors in these models. Acta Crystallogr A 47:110–119.

Kakuta Y, Pedersen LG, Carter CW, Negishi M, Pedersen LC. 1997. Crystal structure of estrogen sulphotransferase. Nat Struct Biol 4:904–908.

Kester MH, Bulduk S, Tibboel D, Meinl W, Glatt H, Falany CN, et al. 2000. Potent inhibition of estrogen sulfotransferase by hydroxylated PCB metabolites: a novel pathway explaining the estrogenic activity of PCBs. Endocrinology 141:1897–1900.

Korach KS, Davis VD, Curtis SW, Bocchinfuso WP. 1997. Xenoestrogens and estrogen receptor action. In: Endocrine Toxicology (Thomas JA, Colby HD, eds). Washington, DC:Taylor and Francis; 181–213.

Korach KS, Sarver P, Chae K, McLachlan JA, McKinney JD. 1988. Estrogen receptor-binding activity of polychlorinated hydroxybiphenyls: conformationally restricted structural probes. Mol Pharmacol 33:120–126.

Kraulis PJ. 1991. MOLSCRIPT: a program to produce both detailed and schematic plots of protein structures. J Appl Crystallogr 24:946–950.

McKinney JD, Gottschalk KE, Pedersen L. 1983. A theoretical investigation of the conformation of polychlorinated biphenyls (PCB's). J Mol Struct THEOCHEM 104:445–450.

McKinney JD, Singh P. 1988. 3,3′,5,5′-Tetrachloro-4,4′-dihydroxybiphenyl. A coplanar polychlorinated biphenyl. Acta Crystallogr Sect C Cryst Struct Commun 44:558.

Merritt EA, Bacon DJ. 1997. Raster3D: photorealistic molecular graphics. Methods Enzymol 277:505–524.

Otwinowski Z, Minor V. 1997. Processing of x-ray diffraction data collected in oscillation mode. Methods Enzymol 276:307–326.

Pedersen LC, Petrotchenko E, Shevtsov S, Negishi M. 2002. Crystal structure of the human estrogen sulfotransferase-PAPS complex: evidence for catalytic role of Ser137 in the sulfuryl transfer reaction. J Biol Chem 277:17928–17932.

Qian YM, Sun XJ, Tong MH, Li XP, Richa J, Song WC. 2001. Targeted disruption of the mouse estrogen sulfotransferase gene reveals a role of estrogen metabolism in intracrine and paracrine estrogen regulation. Endocrinology 142:5342–5350.

Schuur AG, Brouwer A, Bergman A, Coughtrie MW, Visser TJ. 1998. Inhibition of thyroid hormone sulfation by hydroxylated metabolites of polychlorinated biphenyls. Chem Biol Interact 109:293–297.

Tong MH, Song WC. 2002. Estrogen sulfotransferase: discrete and androgen-dependent expression in the male reproductive tract and demonstration of an in vivo function in the mouse epididymis. Endocrinology 143:3144–3151.

Zhang H, Varlamova O, Vargas FM, Falany CN, Leyh TS, Varmalova O. 1998. Sulfuryl transfer: the catalytic mechanism of human estrogen sulfotransferase. J Biol Chem 273:10888–10892.